

Simulation of Ultra-High Energy Photon Propagation in the Geomagnetic Field

P. Homola^{a,*}, D.Góra^a, D. Heck^b, H. Klages^b, J. Pękala^a,
M. Risse^b, B. Wilczyńska^a, and H. Wilczyński^a

^a*Institute of Nuclear Physics PAS, Kraków, ul. Radzikowskiego 152, 31-342
Kraków, Poland*

^b*Forschungszentrum Karlsruhe, Institut für Kernphysik, 76021 Karlsruhe,
Germany*

Abstract

The identification of primary photons or specifying stringent limits on the photon flux is of major importance for understanding the origin of ultra-high energy (UHE) cosmic rays. We present a new Monte Carlo program allowing detailed studies of conversion and cascading of UHE photons in the geomagnetic field. The program named PRESHOWER can be used both as an independent tool or together with a shower simulation code. With the stand-alone version of the code it is possible to investigate various properties of the particle cascade induced by UHE photons interacting in the Earth's magnetic field before entering the Earth's atmosphere. Combining this program with an extensive air shower simulation code such as CORSIKA offers the possibility of investigating signatures of photon-initiated showers. In particular, features can be studied that help to discern such showers from the ones induced by hadrons. As an illustration, calculations for the conditions of the southern part of the Pierre Auger Observatory are presented.

Key words: ultra-high energy cosmic rays, extensive air showers, geomagnetic

cascading, gamma conversion

PACS: 13.85.Tp, 95.85.Ry, 96.40.Pq, 98.70.Sa

** Corresponding author:* tel.: +48 12 6628348, fax: +48 12 6628012
Email address: Piotr.Homola@ifj.edu.pl (P. Homola).

1 Program Summary

CPC Program Library Index: 1.1 Cosmic Rays

Title of program: PRESHOWER 1.0

Catalog number:

Program obtainable: from P. Homola, e-mail: Pi-
otr.Homola@ifj.edu.pl

Computer on which the program has Intel-Pentium based PC
been thoroughly tested:

Operating system: Linux, DEC-Unix

Programming languages used: C, FORTRAN 77

Memory required to execute: < 100 kB

No. of bits in a word: 32

Has the code been vectorized? no

Number of lines in distributed program: 1900

Other procedures used in IGRF [1], bessik, ran2 [2]
PRESHOWER:

Nature of physical problem: simulation of a cascade of particles initiated by UHE photon passing through the geomagnetic field above the Earth's atmosphere.

Method of solution:

The primary photon is tracked until its conversion into e^+e^- pair or until it reaches the upper atmosphere. If conversion occurred each individual particle in the resultant preshower is checked for either bremsstrahlung radiation (electrons) or secondary gamma conversion (photons). The procedure ends at the top of atmosphere and the shower particle data are saved.

Restrictions on the complexity of the problem:

gamma conversion into particles other than electron pair hasn't been taken into account

Typical running time:

100 preshower events with primary energy 10^{20} eV require a 800 MHz CPU time of about 50 min., with 10^{21} eV the simulation time for 100 events grows up to 500 min.

2 Introduction

The existence of ultra-high energy cosmic rays (UHECR) beyond the Greisen-Zatsepin-Kuzmin (GZK) cutoff energy [3] is one of the main puzzles in today’s astrophysics. The composition of UHECR, if known, could provide a stringent test of models of particle acceleration and propagation towards the Earth. Most theoretical efforts are made towards explaining the acceleration of protons to ultra-high energies. This is because protons seem to be the most promising candidates for the UHECR particles. There are, however, also so-called exotic models which postulate decays of supermassive “X-particles”. A common prediction of these models is that there should be a significant photon flux in the ultra-high energy region. Accurate identification of photon primaries, measurement of the ultra-high energy photon flux, or specifying the upper limit for it, will provide an excellent test for the models of cosmic-ray origin.

Ultra-high energy photons in the presence of the geomagnetic field can convert into an electron-positron pair before they enter the atmosphere. Synchrotron radiation of this pair gives rise to a cascade of photons. Some of them can have energies sufficient for the next conversion. The cascade at the top of the atmosphere thus consists mainly of photons and two or more electrons. We will call this cascade a “preshower” since it originates and develops above the upper atmosphere, i.e. before the “ordinary” shower development in the air.

Particles of a preshower induce subshowers after entering the atmosphere. A superposition of these subshowers will be seen by detectors as one extensive air shower, whose profile is expected to differ from the profile of a shower induced by a single unconverted photon.

Forthcoming experiments with large collecting apertures (Pierre Auger Observatory [4], EUSO [5]), that are designed to detect cosmic rays of ultra-high energies, give a good opportunity to test these models. A photon-induced shower might have observable features that allow to distinguish it from showers initiated by hadrons.

In this paper we describe the PRESHOWER program that allows extensive studies of properties of photon-induced showers. The program performs a simulation of the propagation of photons before they enter the Earth's atmosphere and can be used both as an independent analysis tool as well as a part of an air shower simulation package (e.g. CORSIKA [6]).

With the PRESHOWER program working in stand-alone mode we performed, as an illustration, an analysis of basic properties of preshower for the magnetic conditions of Malargüe in Argentina – the site of the Southern Pierre Auger Observatory [4]. The results of these studies, which are presented in Sec. 5, are in general agreement with other analyses [7,8,9,10].

By linking our program to an air shower simulation code one is able to study showers initiated by various primaries. We checked this by combining our PRESHOWER code with the CORSIKA air shower simulation package which simulates air showers initiated by the preshower particles. We simulated photon-induced showers of different energies and different directions at the Southern Pierre Auger Observatory. Although the interaction in the geomagnetic field changes significantly the shower properties so that primary photon events look more similar to hadronic showers, a discrimination between primary photons and hadrons still seems possible.

The plan of the paper is the following: The relevant effects and the formulas applied in the simulation are summarized in Section 3. The structure of the

program is discussed in Section 4. As an illustration, in Section 5 results obtained with the code for the case of the Auger Observatory are discussed. The paper is concluded in Section 6.

3 Preshower physics

At energies above 10 EeV, in the presence of the geomagnetic field, a photon can convert into an e^+e^- pair before entering the atmosphere. The resultant electrons will subsequently lose their energy by magnetic bremsstrahlung. The emitted photons can convert again if their energy is high enough. In this way, instead of one high energy photon at the top of atmosphere, a number of less energetic particles, mainly photons and a few electrons, will emerge constituting a preshower. A superposition of subshowers induced by these particles should be seen by detectors as one extensive air shower which reaches its maximum earlier than a shower induced by a single photon of the same primary energy. This is also due to the Landau-Pomeranchuk-Migdal (LPM) effect [11] which is stronger for photons of higher energies. Both photon conversion and magnetic bremsstrahlung are strongly dependent on the transverse component of the geomagnetic field. In the following, we concentrate on these effects, give the main formulas and discuss their application.

3.1 Geomagnetic field model

Since the geomagnetic field is responsible both for gamma conversion and for bremsstrahlung of electrons, it is very important to model it with adequate accuracy. We use the International Geomagnetic Reference Field model (IGRF) [12] for $n = 10$, n being the highest order of spherical harmonics in the

scalar potential. To calculate the field according to the IGRF model we use the numerical procedures written by Tsyganenko [1]. When choosing $n = 1$, the output of these procedures is equivalent to a dipole model with $|\mathbf{M}| = 8 \cdot 10^{25}$ G·cm³ and with poles at 79.3°N, 71.5°W and 79.3°S, 108.5°E [12].

3.2 Magnetic pair production: $\gamma \rightarrow e^+ e^-$

The number of pairs created by a high-energy photon in the presence of a magnetic field per path length dr can be expressed in terms of the attenuation coefficient $\alpha(\chi)$ [13]:

$$n_{pairs} = n_{photons} \{1 - \exp[-\alpha(\chi)dr]\} \quad (1)$$

where

$$\alpha(\chi) = 0.5(\alpha_{em}m_e c/\hbar)(B_\perp/B_{cr})T(\chi) \quad (2)$$

with α_{em} being the fine structure constant, $\chi \equiv 0.5(h\nu/m_e c^2)(B_\perp/B_{cr})$, B_\perp is the magnetic field component transverse to the direction of the photon's motion, $B_{cr} \equiv m_e^2 c^3/e\hbar = 4.414 \times 10^{13}$ G and $T(\chi)$ is the magnetic pair production function. $T(\chi)$ can be well approximated by:

$$T(\chi) \cong 0.16\chi^{-1}K_{1/3}^2\left(\frac{2}{3\chi}\right), \quad (3)$$

where $K_{1/3}$ is the modified Bessel function of order 1/3. For small or large arguments $T(\chi)$ can be approximated by

$$T(\chi) \cong \begin{cases} 0.46 \exp(-\frac{4}{3\chi}), & \chi \ll 1; \\ 0.60\chi^{-1/3}, & \chi \gg 1. \end{cases} \quad (4)$$

Representative values of $T(\chi)$ are listed in Table 1.

We use Eq. (1) to calculate the probability of γ conversion over a small path length dr :

$$p_{conv}(r) = 1 - \exp[-\alpha(\chi(r))dr] \simeq \alpha(\chi(r))dr \quad (5)$$

and the probability of γ conversion over a longer distance R :

$$P_{conv}(R) = 1 - \exp\left[-\int_0^R \alpha(\chi(r))dr\right] \quad (6)$$

3.3 Magnetic bremsstrahlung

After photon conversion, the electron-positron pair propagates. The energy distribution in an e^+e^- pair is computed according to Ref. [14]:

$$\frac{d\alpha(\varepsilon, \chi)}{d\varepsilon} \approx \frac{\alpha_{em} m_e c B_\perp}{\hbar B_{cr}} \frac{3^{1/2}}{9\pi\chi} \frac{[2 + \varepsilon(1 - \varepsilon)]}{\varepsilon(1 - \varepsilon)} K_{2/3} \left[\frac{1}{3\chi\varepsilon(1 - \varepsilon)} \right], \quad (7)$$

where ε denotes the fractional energy of an electron and the other symbols were explained in the previous chapter. The probability of asymmetric energy partition grows with the primary photon energy and with the magnetic field. Beginning from $\chi > 10$, the asymmetric energy partition is even more favored than the symmetric one.

Electrons traveling at relativistic speeds in the presence of a magnetic field emit bremsstrahlung radiation (synchrotron radiation). For electron energies $E \gg m_e c^2$ and for $B_\perp \ll B_{cr}$, the spectral distribution of radiated energy is given in Ref. [15]:

$$f(y) = \frac{9\sqrt{3}}{8\pi} \frac{y}{(1 + \xi y)^3} \left\{ \int_y^\infty K_{5/3}(z)dz + \frac{(\xi y)^2}{1 + \xi y} K_{2/3}(y) \right\} \quad (8)$$

where $\xi = (3/2)(B_\perp/B_{cr})(E/m_e c^2)$, E and m_e are electron initial energy and rest mass respectively, $K_{5/3}$ and $K_{2/3}$ are modified Bessel functions, and y is related to the emitted photon energy $h\nu$ by

$$y(h\nu) = \frac{h\nu}{\xi(E - h\nu)} ; \quad \frac{dy}{d(h\nu)} = \frac{E}{\xi(E - h\nu)^2} \quad (9)$$

The total energy emitted per unit distance is (in CGS units)

$$W = \frac{2}{3}r_0^2 B_\perp^2 \left(\frac{E}{m_e c^2} \right)^2 \int_0^\infty f(y) dy \quad (10)$$

with r_0 being the classical electron radius. For our purposes we use the spectral distribution of radiated energy defined as

$$I(B_\perp, E, h\nu) \equiv \frac{h\nu dN}{d(h\nu) dx} , \quad (11)$$

where dN is the number of photons with energy between $h\nu$ and $h\nu + d(h\nu)$ emitted over a distance dx . From Eqs. (8), (9), (10), and (11) we get ¹

$$I(B_\perp, E, h\nu) = \frac{2}{3}r_0^2 B_\perp^2 \left(\frac{E}{m_e c^2} \right)^2 f(h\nu) \frac{E}{\xi(E - h\nu)^2} . \quad (12)$$

Provided dx is small enough, dN can be interpreted as a probability of emitting a photon of energy between $h\nu$ and $h\nu + d(h\nu)$ by an electron of energy E over a distance dx . In our simulations we use a small step size of $dx = 1$ km. The total probability of emitting a photon in step dx can then be written as

$$P_{brem}(B_\perp, E, h\nu, dx) = \int dN = dx \int_0^E I(B_\perp, E, h\nu) \frac{d(h\nu)}{h\nu} . \quad (13)$$

¹ Expression (12), valid for all values of $h\nu$, is equivalent to Eq. (2.5a) in Ref. [13]. A simplified form of distribution (12) is given by Eq. (2.10) in Ref. [13], however it can be used only for $h\nu \ll E$.

The shape of the bremsstrahlung spectrum for two different energies is shown in Fig. 1. The three curves in each plot correspond to different values of the transverse magnetic field: 0.3 G, 0.1 G and 0.03 G from the uppermost to the lowest curve respectively. The energy of the emitted photon is simulated according to the probability density distribution $dN/d(h\nu)$ obtained from Eq. 13.

3.4 Related physics topics

In this section we shortly discuss the importance of other physics effects connected to our main subject. These are:

- The geomagnetic field deflects the electrons from the initial preshower direction. To evaluate this deflection we use the equation

$$\frac{m_{rel}v^2}{R} = evB_{\perp}; \quad m_{rel} = \frac{E}{c^2} \quad (14)$$

where v is the speed of electron and e is the elementary charge, to find the radius of curvature R . If R is much larger than the electron path length L and assuming constant values of B_{\perp} , E and $v \approx c$, the linear displacement from the preshower core in the plane perpendicular to the initial direction is well approximated by:

$$\Delta x \cong \frac{L^2}{2R} = \frac{ecB_{\perp}L^2}{E} \quad (15)$$

For typical values like $B_{\perp} = 0.1$ G, $L = 1000$ km (see Section 5) and relatively small energy of $E = 10^{18}$ eV, we get $R \approx 10^{11}$ km which gives $\Delta x \cong 0.5$ cm. Assuming a larger value for L , one should keep in mind that at higher altitudes \mathbf{B} is lower and E is higher. Allowing for other possible combinations of B_{\perp} , E and L one comes to a very safe conclusion that in any case $\Delta x < 1$ m.

- The initial angular spread of particles in both pair production and bremsstrahlung can be approximated by $\Delta\theta \simeq m_e/E$ [16]. Even for energies as low as 10^{18} eV one has $\Delta\theta \approx 10^{-12}$ which even for extremely long paths like for instance 10000 km results in negligible linear deviations at the top of the atmosphere of $\Delta x \approx 10^{-3} \text{ cm}$.
- A γ -ray traveling through the vicinity of the Sun can cascade in the magnetosphere of the Sun where the field is much stronger than near the Earth. The particles originated in conversion near the Sun can be significantly deflected from their initial direction by the solar magnetic field. The cascade of such particles after reaching the Earth's atmosphere will induce an air shower of large lateral extent which might be well distinguishable from proton or iron showers. However, the predicted rate of such events for primary energies of order 10^{19} eV is very low: about 1 event per 10 years for the Pierre Auger Observatory [17]. In our simulations we do not consider cascading in the Sun's magnetosphere.
- The magnetic field embedded in the solar wind is of order 10^{-5} G [18] and it influences the Earth's magnetosphere at altitudes of order $8-10R_\oplus$. Even for a primary energy as high as 10^{21} eV gamma conversion takes place within $2R_\oplus$ above the sea level (see Section 5) where the Earth magnetic field is not less than 10^{-2} G. Thus, the solar wind can be neglected in our studies.
- The preshower electrons traveling at speeds $v < c$ are delayed with respect to the photons. This delay however is very small and can be neglected. For an extreme case of a 10^{18} eV electron traveling a path of 20000 km, the delay is of order 10^{-26} s. The delay of the particles not parallel to the main direction is also negligible (see the above discussion on the lateral spread of a preshower).

4 Structure of the program

The following subsections refer to the stand-alone mode of the PRESHOWER program. The PRESHOWER-CORSIKA mode requires only the main procedure generating events, `preshw`, which is described in subsection 4.3. All the input data in the PRESHOWER-CORSIKA mode are provided via the main CORSIKA input file, the standard output is printed within the CORSIKA output, and the `multirun.dat` file is not returned, since there is only one run per one primary trajectory allowed in CORSIKA. There is also a different random number generator used in the PRESHOWER-CORSIKA mode than in the stand-alone one. For more information on the PRESHOWER-CORSIKA mode the user can refer to the latest CORSIKA manual [19] or contact the corresponding author.

4.1 The source code and other files in the PRESHOWER packet

The PRESHOWER code consists of the following files:

preshw.c contains the main procedure generating preshowers, `preshw`, and the other procedures in C that are called by `preshw`.

prog.c is used only in the stand-alone mode. It reads the input file `INPUT` and calls the preshower procedure `preshw`.

igrf.f is an external procedure for calculation of the geomagnetic field according to the IGRF model (author: N.A.Tsyganenko [1]), it is called by `preshw`.

rmmard.f is a dummy Fortran routine used only in the stand-alone version for the proper linking of the program. In the PRESHOWER-CORSIKA mode the actual `rmmard` is responsible for random number generation.

For the user's convenience there are some more files included in the PRESOWER packet:

Makefile compilation and linking commands under linux.

README.txt short information on the content of the PRESOWER packet and on the installation process.

INPUT typical input data read by the program working in the stand-alone mode. In the PRESOWER-CORSIKA mode all the input data required by `preshw` are read directly from the main CORSIKA input file.

part_out.dat the example of a detailed output file containing information on the preshower particle data being the result of running the program with the input **INPUT**.

multirun.dat the example of an output file summarizing the program run with the input **INPUT**; this file is produced only in the stand-alone mode.

out.txt the standard output produced by the program in the stand-alone mode with the use of the input data from **INPUT**.

4.2 Input and output data

The input data are read by the main program from the file **INPUT** and then passed to the `preshw` procedure. These data are

- (1) the primary photon energy, [GeV]
- (2) the zenith angle of the shower trajectory in the local reference frame (see Sec. 5), [deg]
- (3) the azimuth angle of the shower trajectory in the local frame, [deg]
- (4) the top of the atmosphere – e.g. the value obtained from CORSIKA, [km a.s.l.]
- (5) geographical position of the observatory: longitude [deg]

- (6) geographical position of the observatory: latitude [deg]
- (7) the year of observation (needed for calculation of the field)
- (8) number of runs

An exemplary set of the input data can be found in the file **INPUT**.

There are two output files produced by the PRESHOWER program: **part_out.dat** and **multirun.dat**. Both files begin with a header containing all the crucial run information, then comes the description of columns and then the data. The data in **part_out.dat** are presented in two columns: particle id (1 - photons, 2 - positrons, 3 - electrons) and particle energy at the top of the atmosphere (in eV). The columns in **multirun.dat** are explained as follows:

- (1) the run number
- (2) altitude of the first photon conversion in km a.s.l.
- (3) total number of particles at the top of the atmosphere
- (4) number of photons
- (5) number of electrons
- (6) maximum electron energy
- (7) maximum photon energy
- (8) fraction of energy carried by electrons
- (9) total energy carried by preshower particles = primary photon energy
- (10) total energy carried by electrons
- (11) total energy carried by photons

The information printed as standard output begins with the same header as the output files and is followed by the specific information on each run (all energies given in eV): the run number, the altitude of each conversion together with the energy partition information, preshower summary at the top of the atmosphere: total energy carried by photons (E_{tot_g}), total energy carried by

electrons (`Etot_e`), maximum photon energy (`Eg_max`), maximum electron energy (`Ee_max`), number of particles (`n_part`), number of photons (`n_phot`), number of positrons (`n_e+`) and number of electrons (`n_e-`). The example of a standard output is the file `out.txt` included in the PRESHOWER packet.

4.3 Generation of events

After reading the input parameters (see Sec.4.2) the event generation procedure `preshw` is called, within which all the calculations are performed. In the initial stage all the necessary parameter transformations are applied and the preshower trajectory vector is computed. The propagation path length is set to be $5R_{\oplus}$ long, which e.g. for vertical showers means the simulation starting altitude of $5R_{\oplus}$ above sea level. All the data concerning the particles in the preshower are stored in the array `part_out` which at the beginning has only one entry: the primary photon. In steps of 10 km the transverse magnetic field is computed by the procedure `B_transverse`, then the probability of conversion is found using Eq. (5). The step size has been checked to be sufficiently small. If the conversion takes place, the particle array is updated by replacing the photon with an e^+ and adding an e^- at the array end. The energy partition fraction is found by the function `ppfrac`. To assure accurate bremsstrahlung simulation, beginning from the first gamma conversion the step of 1 km is used for all particle types. In every step, for each photon in the array, we check again for the conversion effect. In case of electrons the bremsstrahlung radiation is simulated using function `brem`. The probability of emitting a photon is calculated from Eq. (13) with the integration starting from $h\nu = 10^{12}$ eV and logarithmic steps of 0.01. Bremsstrahlung photons of energies lower than 10^{12} eV have a very small influence on the air shower evolution (see also Section 5) and hence they are neglected.

Once a bremsstrahlung photon is emitted, its energy is determined by the probability distribution $dN/d(h\nu)$ obtained again from Eq. (13), and the energy of the radiating electron is diminished correspondingly. Simulations are finished when the (adjustable) altitude of the top of the atmosphere is reached and all preshower particle parameters are written out (in the stand-alone mode) or passed to CORSIKA.

4.4 *Compilation, linking and running the program*

In order to compile, link and run PRESOWER under Linux one should first create a file **nr_fun.c** in the PRESOWER home directory and place the header:

```
#include <stdio.h>
#include <math.h>
```

at the beginning of this file. Then, below the header, the source code of the Numerical Recipes [2] procedures **ran2** and **bessik** (together with the procedures called by **bessik**: **beschb**, **chebev** and **nrerror**) should be pasted. To compile and link the program one just types “make” in the PRESOWER home directory. For Unix compilation and linking one needs to replace the proper commands in Makefile. Once the data in the **INPUT** file are appropriate, the program can be started by typing “./preshower”. The compilation and linking process can be verified by running the program with the exemplary **INPUT** file included in the packet. If the program runs correctly, it should return the same output files as those included in the packet (**part_out.dat**, **multirun.dat**) and the standard output as in **out.txt**.

5 Illustration of preshower simulations

The results presented in the following are obtained for the magnetic conditions of the Southern Auger Observatory in Malargüe, Argentina (35.2°S , 69.2°W). Other geographical positions could easily be adopted. The shower trajectories are given in the local frame where the azimuth increases in the counter-clockwise direction and $\phi = 0^{\circ}$ means a shower coming from the geographical North.

To visualize how the transverse magnetic field (B_{\perp}) can change along the shower trajectory, we have chosen some representative directions along which a particle encounters B_{\perp} of significantly different strengths: strong, medium and weak. The “strong field direction” is the one along which B_{\perp} is maximal compared to other directions with zenith angles $\theta \leq 60^{\circ}$ and is defined by the angles $\theta = 60^{\circ}$ and $\phi = 177^{\circ}$. Similarly, the weak B_{\perp} trajectory (“weak field direction”) was chosen to resemble the local field direction at Malargüe of $\theta = 50^{\circ}$, $\phi = 357^{\circ}$ [12]. The “medium field direction” is a vertical trajectory ($\theta = 0^{\circ}$). In the following we will refer to these directions.

5.1 Geomagnetic cascading

In Fig. 2 we show how B_{\perp} changes with altitude for the strong, medium and weak field directions. The trajectories end at the chosen top of the atmosphere. In addition to the altitude dependence of B_{\perp} , large directional differences are visible. Of course we expect the strong field direction to coincide with the direction of a stronger preshower effect.

In Fig. 3, the altitudes of first photon conversion are shown for different energies in the strong field direction. The percentage values shown for each curve

denote the total conversion probability up to the top of atmosphere, which is adjusted here to the starting altitude of CORSIKA at 112 km. It can be seen that for the magnetic field above Malargüe, the pair production effect becomes important for energies above 5×10^{19} eV. For all energies of interest, even in case of photons at 10^{21} eV, the conversion altitude is not higher than 13000 km, i.e. about $2R_{\oplus}$ a.s.l. Thus, the range of interest of the magnetic field strength for the case of Malargüe is $0.3 \text{ G} \div 0.01 \text{ G}$ (see Fig. 2).

The distribution plotted in Fig. 3 is consistent with the results of Ref. [7]. The integrated conversion probability computed with Eq. (6) for different γ energies and for the two trajectories of strong and weak field directions is plotted in Fig. 4. For photons of energies between 5×10^{19} eV and 5×10^{20} eV a change in the arrival direction, i.e. a change in the magnetic field component perpendicular to the photon trajectory, may imply a dramatic increase or decrease of the conversion probability. Thus, for these energies we expect a strong directional dependence of the preshower effect which might serve as characteristic fingerprint of photons as primary cosmic rays.

The directional dependence of the gamma conversion probability is shown in more detail in Fig. 5 for different arrival directions and primary energies. The conversion effect starts to be important for directions towards the magnetic South pole at photon energies around 50 EeV. For energies of about 150 EeV the conversion is very probable for almost every direction. The photons coming from azimuthal angles around 150° at large zenith angles convert more likely than the others. To explain this, one notes that for a given altitude the magnetic field is strongest around the geomagnetic axis and of course the field becomes stronger with decreasing altitude. Since the photons coming from the geomagnetic South, which corresponds to the azimuth about 150° in case of Malargüe, cross the very vicinity of the geomagnetic axis, they must encounter

the stronger magnetic field than the others and hence their conversion probability is higher. The larger zenith angle for these photons means that the strong field region is crossed at the lower altitudes where the field is stronger and the conversion process is more effective. The plots in Fig. 5 are consistent with the values given in Ref. [10].

All the preshower discussed here are presented in their final stage of development at the “top of the atmosphere” which in our simulations is assumed to be 112 km a.s.l. – where in the CORSIKA code shower simulations are started.

In Fig. 6 mean energy spectra are plotted for 1000 preshower initiated by photons of energy 10^{20} eV arriving at the top of atmosphere from the strong field direction for Malargüe. In the top row we show the distribution of photons (left) and the distribution of photons weighted by their energies (right). We start the simulations of the bremsstrahlung radiation for the energy threshold of 10^{12} eV so the photons of lower energies are absent in the distribution. In this way we take into account the majority of the photons even if those of energies lower than 10^{16} eV may have little impact on the longitudinal profile of the resultant air shower. The total energy fraction carried by such photons is very low (see the top right plot in Fig. 6) and the induced subshowers fade very quickly. In the simulation run presented in Fig. 6, only 78 out of 1000 primary photons did not convert into e^+e^- , these are seen in the top right plot as the narrow peak at $E = 10^{20}$ eV.

The distributions of the electrons in the same sample of 1000 preshower are shown in the bottom row of Fig. 6. Again, the spectrum of particles is plotted to the left and the spectrum weighted by energy to the right. Only in three cases out of 1000 a bremsstrahlung photon converted into e^+e^- so the total number of electrons is 1850 and not 1844. When the conversion happens

at a lower altitude, the electrons radiate less bremsstrahlung before entering the atmosphere. These cases are seen in the spectrum as a tail towards high energies.

Some characteristics of the preshower shown in Figure 6 are summarized in Table 2 together with some other exemplary preshower cases. The conversion probabilities are consistent with those in Figure 5. For higher initial energies gamma conversion takes place at higher altitudes (see Fig. 3) and the resultant electrons radiate more bremsstrahlung photons so the number of particles is larger. Additionally for energies as high as 10^{21} eV there is more than one gamma conversion per each preshower which also enlarges N_{part} . Comparing strong B_{\perp} and weak B_{\perp} directions for a given energy, the large directional dependence of preshower evolution can be noted. In case of $E_0 = 10^{20}$ eV from the weak B_{\perp} direction we expect unconverted photons initiating cascades with a large depth of shower maximum X_{max} due to the LPM effect. The strong B_{\perp} forces the initial energy to be split into about 500 particles of which the highest energy particle typically is a photon with the energy about 5 times lower than the initial one. This means that the longitudinal profile of the resultant air shower will have the maximum higher in the atmosphere, which will make it more similar to a proton-like profile. The energy splitting in this case will compete with the LPM effect. This splitting effect for $E_0 = 10^{21}$ eV for the strong B_{\perp} direction is even more dramatic: the highest energy particle in the preshower is more than 16 times less energetic than the primary photon. The maximum γ energy in the preshower for the weak field direction is higher than for the strong field since the conversion probability is lower in a weaker field (see Fig. 4). Detailed distributions of $\langle N_{part} \rangle$, $\langle N_{e^+e^-} \rangle$, $\langle \max E_{\gamma} \rangle$ and $\langle \max E_e \rangle$ for $E_0 = 10^{21}$ eV and the strong B_{\perp} are shown in the top left, top right, bottom left and bottom right plots of Figure 7, respectively.

As mentioned above, the number of particles in the preshower is connected to the altitude of the first gamma conversion. This correlation is presented in Figure 8. The higher altitude of conversion gives more particles at the top of the atmosphere because the electron-positron pair radiates bremsstrahlung over a longer path. The increase in particle number is slightly larger at low altitudes because of the stronger magnetic field.

For the same reasons the total energy fraction carried by the electrons should be smaller for higher conversion altitudes. This dependence is shown in Figure 9. One notes that for high altitudes of the first conversion only about 1% of the initial energy of 10^{20} eV remains in the electrons at the top of the atmosphere, while all the rest is radiated into photons. With decreasing altitudes the energy radiated into photons decreases. The three points in excess of the general trend in Figure 9 are the cases where the primary photon converted at high altitude and one of the resulting bremsstrahlung photons converted close to the top of the atmosphere - at 228, 442 and 133 km a.s.l respectively for the points from right to left. The threshold for γ conversion in this case is about $5 \cdot 10^{19}$ eV, so at least one member of e^+e^- pair had an initial energy greater than 10^{19} eV, and since its birth altitude was relatively low, there was little time for radiation.

5.2 Atmospheric cascading: PRESHOWER and CORSIKA

The results presented above give a general idea about the characteristics of preshowers initiated by UHE photons before entering the atmosphere. The next step is to simulate air showers induced by different preshowers or unconverted photons and compare the results with the proton-induced showers in order to investigate the signatures of UHE photons that will be measurable.

able by the Pierre Auger Observatory. For this purpose we connected the PRESOWER program to CORSIKA, a commonly used air shower simulation code.

The connection between the two codes is organized as follows. First, the distribution of the preshower particles at the top of the atmosphere is simulated with the original preshower code, then the output is passed to CORSIKA and finally the resulting air shower is simulated as a superposition of the subshowers initiated by the preshower particles.

Electromagnetic interactions are simulated in CORSIKA using an adapted version [20] of the EGS4 code [21], which includes the Landau-Pomeranchuk-Migdal effect [11]. To reduce the computational effort in CPU time, the technique of particle thinning [22], including weight limitation [23,24], is applied. More specifically, a thinning level of 10^{-5} has been chosen, and particle weights are limited to $10^{-5}E_0/\text{GeV}$, with E_0 being the primary energy. This keeps artificial fluctuations introduced by the contribution of individual particles sufficiently small for the analysis of shower maximum depths [25].

In Table 7 we compare X_{max} and RMS of X_{max} for gamma induced showers of different primary energies and arrival directions. The X_{max} of proton-induced showers using the high-energy hadronic interaction model QGSJET 01 [26] is 820 (870) g/cm² for 10^{20} (10^{21}) eV, and using the SIBYLL 2.1 model [27] 855 (915) g/cm². The RMS in all cases is about 50–60 g/cm². Both for $E_0 = 5 \cdot 10^{19}$ eV in strong B_\perp direction and for $E_0 = 10^{20}$ eV in weak B_\perp direction, almost every photon remains unconverted when entering the atmosphere, resulting in deep $\langle X_{max} \rangle$ and large fluctuations due to the LPM effect. A comparison to the longitudinal profile of hadronic primaries shows that unconverted primary photons might be well distinguishable from primary

protons or nuclei even on event-by-event basis.

Almost all the photons at 10^{20} eV arriving from the strong field direction convert into e^+e^- pairs. As the most energetic bremsstrahlung photons have energies several times lower than the primary photon energy, the subshowers develop faster. On average, the showers reach their maxima earlier than the one induced by an unconverted photon, but still not as early as hadronic showers. For larger statistics of 10^{20} eV events and if a substantial fraction of UHE cosmic rays are photons, one expects to see, as described above, the directional anisotropy in $\langle X_{max} \rangle$ and $\text{RMS}(X_{max})$ and on this basis one may draw conclusions on the primary composition. The absence of this dependence would allow us to set upper limits on the photon flux.

At the primary energy of 10^{21} eV all photons convert, whatever the arrival direction. We still see the directional dependence of $\langle X_{max} \rangle$ but it is not as pronounced as previously. The fluctuations of X_{max} in this case are significantly lower (by about a factor 4) than for 10^{20} eV primaries. Table 7 shows that at 10^{21} eV it is more difficult to distinguish a photon primary on the basis of the X_{max} value from a proton one on an event-by-event basis. It is interesting, however, to note the directional dependence of the elongation rate. From Table 7 we see that at Malargüe, for the strong B_\perp direction, the elongation rate of photon-induced showers between 10^{20} eV and 10^{21} eV is much less than for proton or iron showers. For the weak B_\perp we even have a *negative* elongation rate. This is because the preshowering effect for photons at 10^{21} eV splits the initial energy into energies less than 10^{20} eV and at this energy level, for the weak B_\perp direction, almost all the primary photons remain unconverted and they induce air showers with deeper X_{max} . Low or negative elongation rates could be an additional good signature of photon showers.

More detailed simulations of the signatures mentioned above will allow us to quantify the expected sensitivity of the Auger experiment to a photon fraction in UHE cosmic ray flux. Also other observables will be studied, especially the muon content and the features of the lateral distribution measured by the surface detector, since for the surface measurements the event sample will be about 10 times more numerous than for the fluorescence detector.

6 Summary

We presented a method for studying the signatures of UHECR gamma showers and the practical implementation of this method in the PRESHOWER program. This program was tested extensively both in stand-alone mode and as a part of CORSIKA and was checked for consistency with results quoted in other publications. The preshower option will be accessible in the future release of CORSIKA.

With the code working in stand-alone mode, we studied the preshower characteristics for different primary energies and arrival directions. The strong directional and energy dependence of the preshower effect requires a concise treatment in the simulations. Anisotropies in the preshower cascade translate into anisotropies of air shower observables such as $\langle X_{max} \rangle$ and $\text{RMS}(X_{max})$. First results obtained with PRESHOWER combined with the CORSIKA air shower simulation code for the conditions of the Auger Observatory confirm the expectation that photon showers can be distinguished from hadron ones. Further analyses including other observables such as the muon shower content are in progress.

The new experiments with large collecting apertures give promising prospects

for acquisition of a substantial amount of extensive air shower data in the UHE range of cosmic-ray spectrum. An important step towards explaining the origin of UHE cosmic rays will be the observation of primary UHE photons or specifying stringent upper limits for the photon flux. This requires a detailed understanding of the UHE photon shower characteristics. The presented PRESHOWER code can serve as tool for such simulations.

7 Acknowledgements

We thank R. Engel, M. Kachelriess, S.S. Ostapchenko for valuable remarks and suggestions.

This work was partially supported by the Polish State Committee for Scientific Research under grant No. PBZ KBN 054/P03/2001 and 2P03B 11024 and by the International Bureau of the BMBF (Germany) under grant No. POL 99/013.

A Compilation of procedures/functions

```
preshw(*id, *E_gamma, *the_loc, *phi_loc, *toa, *glong, *glat,
igrf_year, *iiprint, *corsika, *nruns, part_out[10000][7],
r_zero, *r_fpp, *N_part_out):
```

This is the main procedure of PRESOWER which simulates the propagation of an UHE photon before its entering the Earth's atmosphere. It takes into account the effect of γ conversion into $e^{+/-}$ pair and subsequent bremsstrahlung radiation of the electrons in the geomagnetic field. As a result a bunch (a preshower) of particles is obtained, mainly photons and a few electrons, instead of the primary photon. The information about all the particles in the preshower is saved (in the stand-alone mode) or returned to CORSIKA (PRESOWER-CORSIKA mode). The output parameters `r_zero`, `r_fpp` and `N_part_out` are required by CORSIKA only – they are not used by the stand-alone version.

INPUT:

- (1) `*id`: primary particle type: always `id=1` (a photon)
- (2) `E_gamma`: primary energy [GeV]
- (3) `*the_loc`, `*phi_loc`: zenith and azimuth angles (in radians) of the shower trajectory given in the local coordinate system
- (4) `*toa`: the top of the atmosphere [cm]
- (5) `*glong`: longitude position of experiment [deg] (Greenwich `glong = 0°`, eastward is positive)
- (6) `*glat`: latitude position of experiment [deg] (North Pole: `glat=90°`, South Pole: `glat=-90°`)
- (7) `*igrf_year`: the year in which the magnetic field is to be computed – this parameter is an input for the `igrf` procedure
- (8) `*iiprint`: print flag (adjustable only in PRESOWER-CORSIKA, in

the stand-alone version `iiprint=1`)

- = 0: suppress printing from `preshw`;
- = 1: enable printing from `preshw`

(9) `*corsika`: mode flag

- = 1: PRESHOWER-CORSIKA: – random generator from CORSIKA is used (`rndm`);
- = 0: stand-alone version: random generator from Numerical Recipes (`ran2`) is used

(10) `*nruns`: number of runs

OUTPUT:

- (1) `part_out[10000][7]`: the array to store the preshower particle data, maximum number of particles: 10000
 - `part_out[n][0]`: particle type: 1 – photon, 2 – e^+ , 3 – e^-
 - `part_out[n][1]`: particle energy [GeV]
 - `part_out[n][2-6]`: not used
- (2) `*r_zero`: height above sea level of the simulation starting point given in [km] above sea level
- (3) `*r_fpp`: height of the first pair production (0 for surviving photons) given in [km] above sea level
- (4) `*N_part_out`: number of preshower particles at the top of the atmosphere (number of entries in `part_out` array)

`bessik(x, xnu, *ri, *rk, *rip, *rkp):`

for argument `x` computes modified Bessel function `rk` of fractional order `xnu`; [2]

`getrand(seed, mode):`

for a given seed `seed` returns a random number from interval (0,1) choosing an appropriate generator according to the `mode` flag: `ran2` for the stand-alone mode (`mode=0`) and `rmmard` for the CORSIKA-PRESHOWER (`mode=1`)

```

float kappa(x):
  an auxiliary function used in the bremsstrahlung procedure brem

brem(B_tr, E_e, E_sg):
  computes bremsstrahlung radiation for the transverse magnetic field B_tr,
  electron energy E_e and bremsstrahlung photon energy E_sg

B_transverse(B, tn):
  getting the geomagnetic field B component which is perpendicular to the
  preshower trajectory tn

ran2(seed):
  the random number generator used only in the stand-alone mode; [2]

cross(a, b, c):
  returns cross product c of vectors a and b

dot(a, b):
  returns dot product of vectors a and b

norm(a, n):
  the input vector a is normalized and returned as vector n

normv(a):
  returns the length of vector a

glob2loc(glob, loc, theta, phi):
  converts global cartesian coordinates glob to the local ones (loc) for the
  geographical position theta (colatitude) and phi (longitude)

sph2car(sph, car):
  converts spherical coordinates sph to the cartesian ones car.

car2sph(car, sph):
  inverse to sph2car

locsphC2glob(locsph, glob, theta, phi, sing, cosgm, sitec):
  converts local spherical coordinates locsph (CORSIKA frame of reference)
  to the global cartesian coordinates glob, using geographical coordinates

```

of the observatory (`theta` - colatitude, `phi` - longitude), global cartesian coordinates of the observatory (`sitec`) and sine and cosine of the declination angle (`sing`, `cosg`)

`ppp(efrac, B_tr, E_g0):`

this auxiliary function is used within `ppfrac`

`ppfrac(s, mode, B_tr, E_g0):`

determines the energy partition after gamma conversion, the computations are performed according to Ref. [14]; `s` - seed, `mode` - determines the type of the random number generator, `B_tr` - transverse magnetic field, `E_g0` - primary photon energy

`igrf_(year, n, r, theta, phi, Br, Btheta, Bphi):`

external Fortran procedure written by Tsyganenko [1]; computes magnetic field according to the IGRF model; used within `b_igrf`; `year` - the year of the experiment, `n` - the highest order of the spherical harmonics in the scalar potential, `r`, `theta`, `phi` - spherical coordinates of the point at which the field is to be found, `Br`, `Btheta`, `Bphi` - spherical coordinates of the magnetic field at given position

`b_igrf(year, r, theta, phi, bcar):`

for a given `year` and position (`r`, `theta`, `phi`) computes the magnetic field `bcar` in global cartesian coordinates according to the IGRF model

`bsph2car(colat, longit, bsph, bcar):`

converts the magnetic field from spherical coordinates (`bsph`) into cartesian ones `bcar`; used only in `b_igrf`

`rndm():`

calls CORSIKA random number generator, used only in the PRESHOWER-CORSIKA mode

References

- [1] N. A. Tsyganenko, National Space Science Data Center, NASA GSFC, Greenbelt, MD 20771, USA
<http://nssdc.gsfc.nasa.gov/space/model/magnetos/data-based/geopack.html>
- [2] Numerical Recipes, <http://www.nr.com>
- [3] K. Greisen, Phys. Rev. Lett. **16**, (1966) 748; G.T. Zatsepin and V.A. Kuzmin, Zh. Eksp. Teor. Fiz. **4**, (1966) 114
- [4] J. Abraham et al., Auger Collaboration, Nucl. Inst. Meth. (2003) submitted; J. Blümer for the Auger Collaboration, J. Phys. G: Nucl. Part. Phys. **29**, (2003) 867
- [5] L. Scarsi et al., *27th Int. Cosmic Ray Conf.*, Hamburg, **2** (2001) 839
- [6] D. Heck, J. Knapp, J.N. Capdevielle, G. Schatz, and T. Thouw, Report FZKA 6019, Forschungszentrum Karlsruhe (1998) (available at www-ik.fzk.de/~heck/corsika/)
- [7] T. Stanev and H.P. Vankov, Phys. Rev. **D55** (1997) 1365
- [8] H.P. Vankov, N. Inoue, and K. Shinozaki, Phys. Rev. **D67** (2003) 043002
- [9] H.P. Vankov, T. Stanev, N. Inoue, A. Misaki, S. Kawaguchi, and E. Konishi, Proc. *28th Int. Cosmic Ray Conf.*, Tsukuba, (2003) 527
- [10] X. Bertou, P. Billoir and S. Dagoret-Campagne, Astropart. Phys. **14** (2000) 121
- [11] L.D. Landau and I.J. Pomeranchuk, Dokl. Akad. Nauk SSSR, **92**, (1953) 535, 735
A.B. Migdal, Phys. Rev. **103**, (1956) 1811
- [12] National Geophysical Data Center, USA, www.ngdc.noaa.gov
- [13] T. Erber, Rev. Mod. Phys. **38** (1966) 626

- [14] J. K. Daugherty, A. K. Harding, *Astrophys. J.* **273** (1983) 761
- [15] A.A. Sokolov, I.M. Ternov, *Radiation from Relativistic Electrons*, Springer Verlag, Berlin, 1986
- [16] M. Sterns, *Phys. Rev.* **76** (1949) 836; A. Borsellino, *Phys. Rev.* **89** (1953) 1023
- [17] W. Bednarek, preprint astro-ph/9911266 (1999)
- [18] www.spaceweather.com
- [19] D. Heck, J. Knapp, available at
www-ik.fzk.de/~heck/corsika/userguide/corsika_tech.html
- [20] D. Heck and J. Knapp, Report **FZKA 6097**, Forschungszentrum Karlsruhe (1998)
- [21] W.R. Nelson, H. Hirayama, and D.W.O. Rogers, Report **SLAC 265**, Stanford Linear Accelerator Center (1985)
- [22] A.M. Hillas, *Nucl. Phys. B (Proc. Suppl.)* **52B** (1997) 29
- [23] M. Kobal, Pierre Auger Collaboration, *Astropart. Phys.* **15** (2001) 259
- [24] M. Rissee, D. Heck, J. Knapp, and S.S. Ostapchenko, *Proc. 27th Int. Cosmic Ray Conf.*, Hamburg (Germany), **2** (2001) 522
- [25] M. Rissee and D. Heck, *Auger Technical Note GAP-2002-043*, www.auger.org, (2002)
- [26] N.N. Kalmykov, S.S. Ostapchenko and A.J. Pavlov, *Nucl. Phys. B (Proc. Suppl.)* **52 B** (1997) 17; D. Heck et al., *Proc. 27th Int. Cosmic Ray Conf.*, Hamburg **1** (2001) 233
- [27] R. Engel, T.K. Gaisser, P. Lipari, and T. Stanev, *Proc. 26th Int. Cosmic Ray Conf.*, Salt Lake City **1** (1999) 415; R.S. Fletcher, T.K. Gaisser, P. Lipari, and T. Stanev, *Phys. Rev. D* **50** (1994) 5710; J. Engel, T.K. Gaisser, P. Lipari, and T. Stanev, *Phys. Rev. D* **46** (1992) 5013

Table 1

The magnetic pair production function $T(\chi)$.

| χ | 0.2 | 0.4 | 1.0 | 5.0 | 10.0 | 30.0 | 100.0 |
|-----------|--------|--------|--------|--------|--------|--------|--------|
| $T(\chi)$ | 5.9e-4 | 1.6e-2 | 9.9e-2 | 2.2e-1 | 2.1e-1 | 1.9e-1 | 1.3e-1 |

Table 2

Exemplary preshower for Malargüe magnetic conditions. For each type of the preshower determined by the initial photon energy E_0 and the arrival direction, in columns 3-7 respectively shown are: the fraction of converting primary photons and the average values (\pm RMS) for the number of particles, the number of electrons, the maximum photon energy and the maximum electron energy. Only converted cases were taken for averaging.

| E_0 [EeV] | direction | fraction converted | $\langle N_{part} \rangle$ | $\langle N_{e^+e^-} \rangle$ | $\langle \text{max}E_\gamma \rangle$ [eV] | $\langle \text{max}E_e \rangle$ [eV] |
|----------------|------------------|-----------------------|----------------------------|------------------------------|--|---|
| 50 | strong B_\perp | 137/1000 | 263 ± 189 | 2.0 ± 0.0 | 6.8 ± 3.2 | 4.9 ± 6.5 |
| 100 | strong B_\perp | 922/1000 | 482 ± 231 | 2.01 ± 0.11 | 18 ± 8 | 2.2 ± 5.3 |
| | weak B_\perp | 0/1000 | 1 | 0 | 100 | 0 |
| 1000 | strong B_\perp | 1000/1000 | 3330 ± 649 | 9.7 ± 2.3 | 65 ± 16 | 4.7 ± 7.1 |
| | weak B_\perp | 1000/1000 | 544 ± 143 | 2.7 ± 1.0 | 167 ± 66 | 7.2 ± 8.3 |

Table 3

X_{max} and RMS values for gamma induced showers of two different primary energies and arrival directions. Here the strong B_{\perp} direction is defined as $\theta = 53^\circ$, $\phi = 177^\circ$ and weak B_{\perp} as $\theta = 53^\circ$, $\phi = 357^\circ$.

| E_0 [eV] | direction | fraction of con- verted | $\langle X_{max} \rangle$ [g/cm ²] | $\langle RMS(X_{max}) \rangle$ [g/cm ²] |
|-------------------|--------------------|----------------------------|--|--|
| $5 \cdot 10^{19}$ | strong B_{\perp} | 1/50 | 1065 | 90 |
| 10^{20} | weak B_{\perp} | 1/100 | 1225 | 175 |
| | strong B_{\perp} | 91/100 | 940 | 85 |
| 10^{21} | weak B_{\perp} | 100/100 | 1040 | 40 |
| | strong B_{\perp} | 100/100 | 965 | 20 |

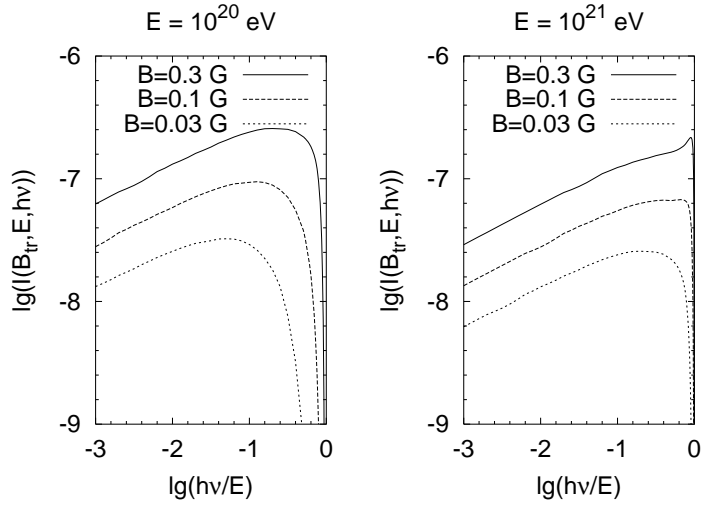


Fig. 1. Bremsstrahlung spectral distribution: $E = 10^{20}$ eV (left) and $E = 10^{21}$ eV (right) for different transverse magnetic field strengths: $B = 0.3$ G, 0.1 G and 0.03 G for the uppermost, middle and lowest curves respectively.

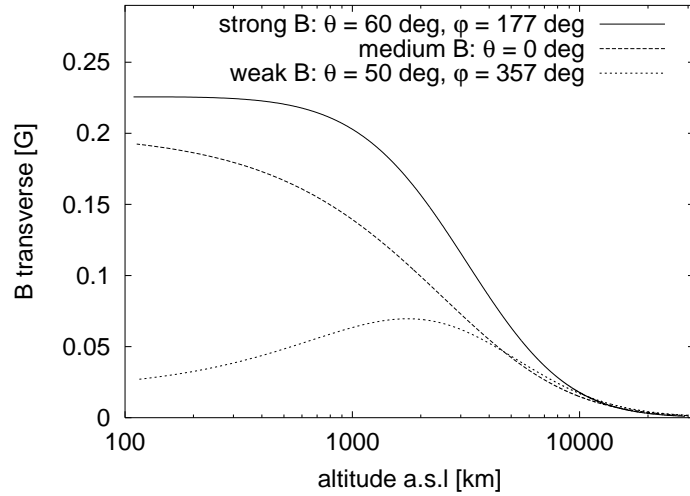


Fig. 2. B_{\perp} along different shower trajectories for the southern Auger Observatory. Curves from top to bottom: strong, medium, and weak field direction (see text).

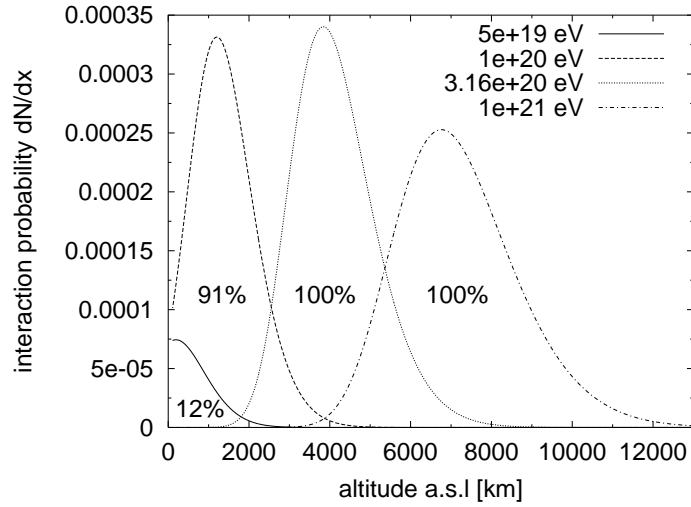


Fig. 3. Altitudes of first conversion along strong field direction at Malargüe plotted for four different primary photon energies. The numbers attached to the curves indicate the total conversion probability (see text).

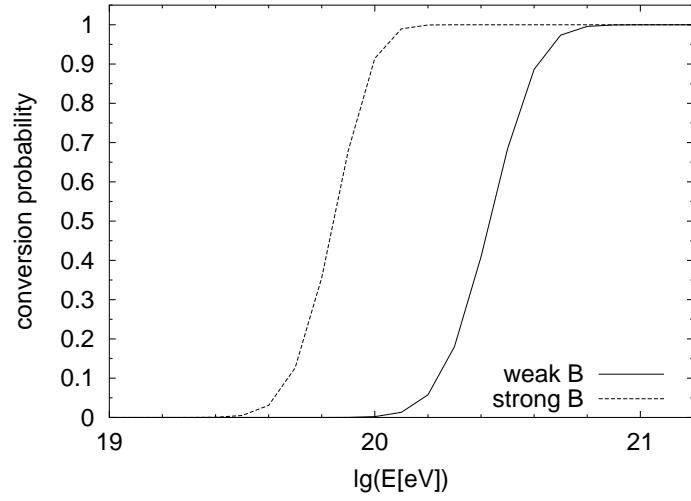


Fig. 4. Integrated conversion probability vs initial γ energy for weak and strong field directions.

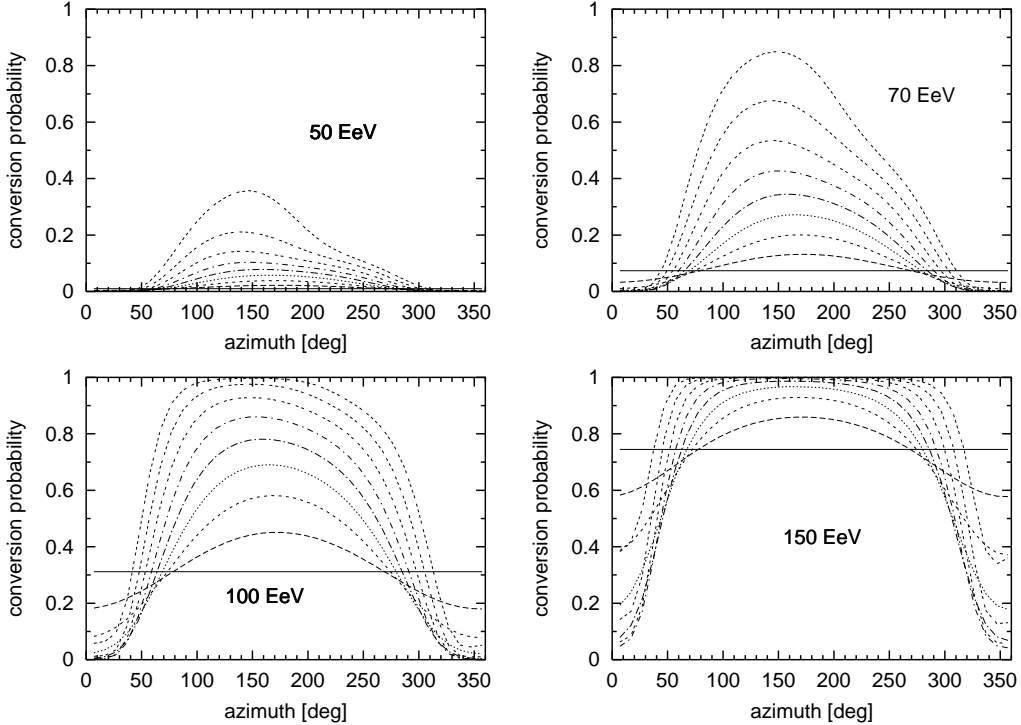


Fig. 5. Total probability of γ conversion for different arrival directions and four initial energies. Each curve corresponds to a different zenith angle: $\theta = 80^\circ$ for the uppermost curve down to $\theta = 0^\circ$ for the lowest one in steps of 10° . Computations are made for Malargüe magnetic conditions and azimuth 0° means the shower arriving from the geographic North.

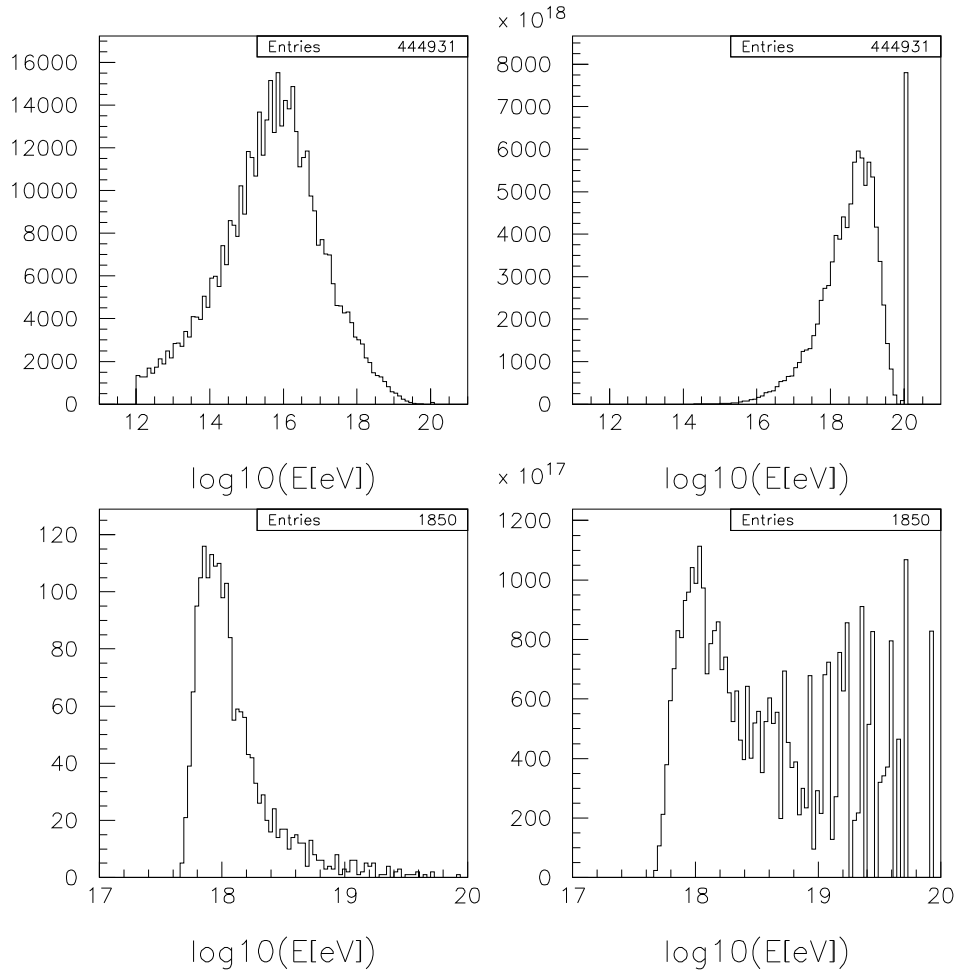


Fig. 6. Energy distribution of photons (top) and electrons (bottom) in 1000 preshowers initiated by 10^{20} eV photons arriving at Malargüe from the strong field direction, compare Table 2. Spectra weighted by energy are plotted to the right.

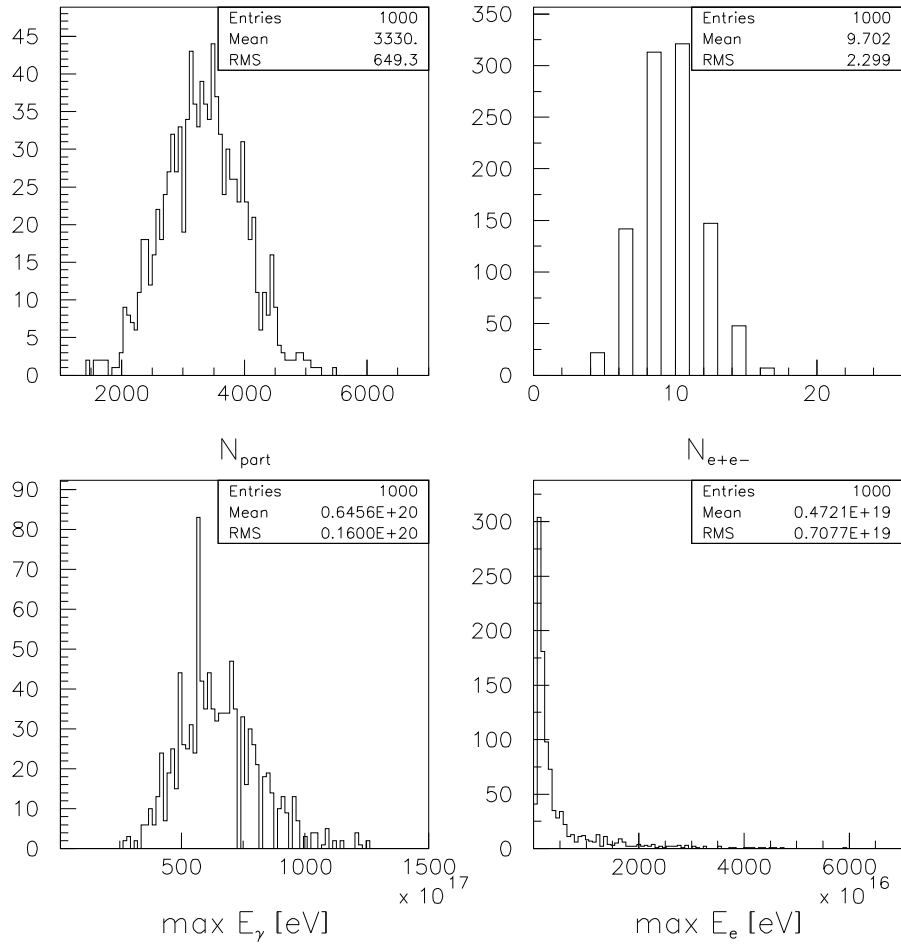


Fig. 7. Distributions of N_{part} (top left), N_{e+e-} (top right), $\max E_\gamma$ (bottom left) and $\max E_e$ (bottom right) for $E_0 = 10^{21}$ eV and the strong B_\perp arrival direction.

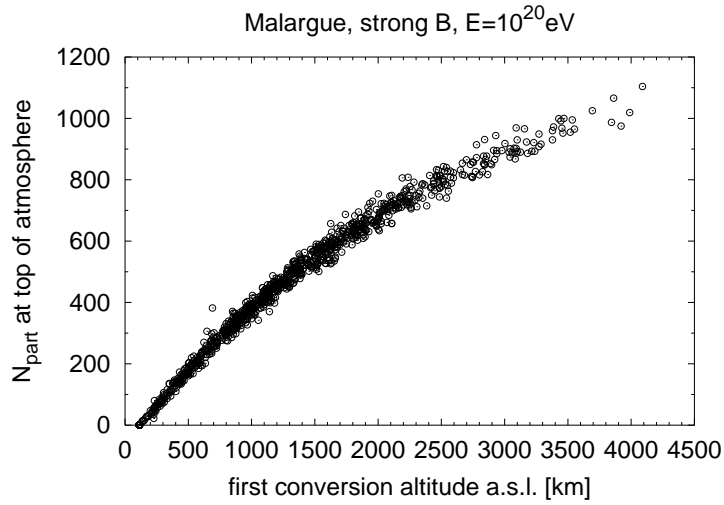


Fig. 8. Number of particles in the preshower for different altitudes of first γ conversion. Plotted are the preshowers initiated by 10^{20} eV photons arriving from the strong B_{\perp} direction.

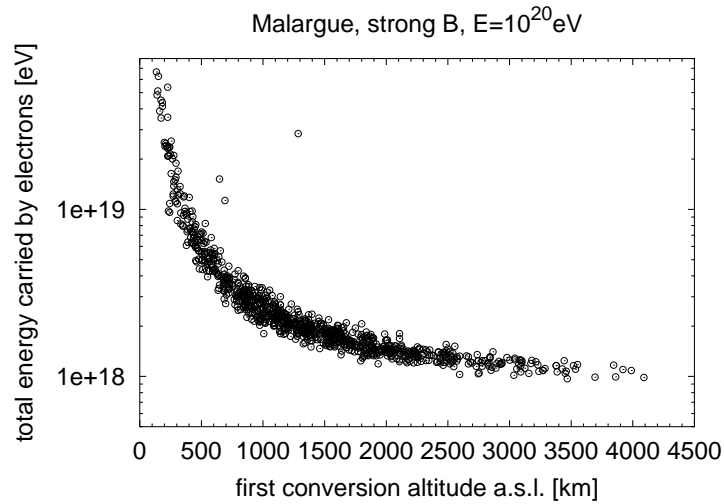


Fig. 9. Energy carried by the preshower electrons at the top of atmosphere vs the altitude of the first γ conversion for a primary photon energy of 10^{20} eV in the strong field direction. The three points in excess of the general trend are the cases where the primary photon converted at high altitude and one of the bremsstrahlung photons converted close to the top of the atmosphere. For further comments see the text.